Results in Physics 10 (2018) 379–384

Contents lists available at ScienceDirect

Results in Physics

journal homepage: www.elsevier.com/locate/rinp

Heat transfer analysis of Prandtl liquid nanofluid in the presence of homogeneous-heterogeneous reactions

Feroz Ahmed Soomro[a], Zafar Hayat Khan[b,*], Rizwan-ul-Haq[c], Qiang Zhang[a]

[a] Department of Mathematics, Nanjing University, Nanjing 210093, China
[b] State Key Laboratory of Hydraulics and Mountain River Engineering, College of Water Resource & Hydropower, Sichuan University, Chengdu 610065, China
[c] Department of Electrical Engineering, Bahria University, Islamabad 40000, Pakistan

ARTICLE INFO

Keywords:
Homogenous-heterogeneous reactions
Nanoparticles
Prandtl fluid
Stretching sheet
Numerical solution

ABSTRACT

The objective of present research work is to analyze the homogeneous-heterogeneous reactions on the MHD two-dimensional stagnation-point flow of non-Newtonian Prandtl fluid flow and heat transfer towards horizontal linear stretching sheet. The governing boundary layer equations using similarity transformation are reduced to ordinary differential equations suitable to be solved using Finite Difference Method. The quantities of interests are thoroughly analyzed under the effects of various emerging parameters. Comparison of the results obtained from limiting case of present model with already existing literature is in good agreement which shows the validity of the present numerical solution. The study concludes that homogeneous and heterogeneous reaction strength decreases the heat transfer rate. On the other hand, Prandtl fluid parameter and elastic parameter increases heat transfer rate.

Introduction

Two main classifications of fluids are Newtonian and non-Newtonian. The later differs from the former in the sense that it does not obey the Newton's law of viscosity. Such types of fluids are encountered by us in our daily life. Honey, paint, toothpaste and fresh concrete are among few of them. For further insight into the study of non-Newtonian fluids and its applications the readers are referred to read the book [1]. So far, the researchers have been engaged in both experimental and mathematical investigation. In present paper we shall present the brief review of various kinds of non-Newtonian models that have been under consideration. Moreover, as a scope of this paper, we shall stick to the non-Newtonian fluid flow over different kinds of stretching surface. The non-Newtonian fluids under investigation are Sisko fluid [2], Casson fluid [3,4], Carreau fluid [5], Maxwell fluid [6], Williamson fluid [7], Oldroyd-B fluid [8], Jeffery fluid [9], second-grade fluid [10].

The focus of present article is on the non-Newtonian Prandtl fluid. Literature survey reveals that not much attention has been pain to the flow and heat transfer characteristics of Prandtl fluid. Akbar et al. [11] studied the MHD stagnation-point flow of Prandtl fluid over shrinking sheet. The numerical solutions revealed the dual mathematical solutions. Soomro et al. [12] considered the Prandtl nanofluid flow to study the passive control of nanoparticle near the horizontal stretching surface. Effect of chemical reactions on the 3D Prandtl fluid over flat surface was studied numerically by Kumar et al. [13].

Chaudhary and Merkin [14] developed a model contains homogeneous-heterogeneous reactions in the two-dimensional stagnation point boundary layer flow. The homogeneous reaction was given by cubic autocatalytic reaction while on the catalyst surface first order reaction was considered. A numerous number of chemical reactions involving such reactions have many practical applications, such as biochemical systems and combustion. Significant studies have been done one the homogeneous-heterogeneous reactions effects on the flow and heat transfer over stretching surface utilizing both Newtonian and non-Newtonian fluid models. Khan et al. [15] considered Casson fluid model to study the homogeneous-heterogeneous reactions on the stagnation-point flow and heat transfer over stretching surface. Williamson fluid flow over convective stretching surface involving homogeneous-heterogeneous reactions was taken into consideration by Ramzan et al. [16]. In another study [17], homogeneous-heterogeneous reactions effects on the flow and heat transfer over stretching cylinder

* Corresponding author.
E-mail address: zafarhayyatkhan@gmail.com (Z.H. Khan).

https://doi.org/10.1016/j.rinp.2018.06.043
Received 12 February 2018; Received in revised form 17 April 2018; Accepted 18 June 2018
Available online 22 June 2018

was analyzed. Non-stagnant Prandlt fluid over the stretching sheet was examined by Khan et al. [18] under the effects of homogenous-heterogeneous reactions. The detailed analysis on the comparison between magnetic and non-magnetic nanoparticles suspended nanofluid flow and heat transfer characteristics under the effects of homogeneous-heterogeneous reactions was carried out by Abbas et al. [19]. Analytical study was carried out by Hayat et al. [20] on the melting heat transfer characteristics of Newtonian viscous fluid over the stretching sheet of variable thickness utilizing the effects of homogeneous-heterogeneous reactions.

Insight into the literature depicts that the homogeneous-heterogeneous reaction effects on the flow and heat transfer of stagnation-point Prandtl fluid flow and heat transfer has not been studied before. So the purpose of present research work is to seek it numerical solution using Finite Difference Method which is analyzed for the quantities of interest against emerging physical parameters.

Mathematical model

Let us consider two-dimensional stagnation-point flow of a Prandlt fluid in the presence of chemical reaction over linear stretching sheet. The fluid is incompressible, steady and confined to cartesian plane ($y > 0$). Fluid flows along positive *y-axis* and meets the plane $y = 0$. Induced magnetic field is neglected due to low Reynolds number in comparison to applied magnetic field normal to the stretching sheet. Geometry of the model is described in Fig. 1. The extra stress tensor for the Prandtl fluid is given by:

$$\tau = \frac{m_1 \arcsin\left(\frac{1}{m_2}\left(\left(\frac{\partial \bar{u}}{\partial y}\right)^2 + \left(\frac{\partial \bar{v}}{\partial x}\right)^2\right)^{1/2}\right)}{\left(\left(\frac{\partial \bar{u}}{\partial y}\right)^2 + \left(\frac{\partial \bar{v}}{\partial x}\right)^2\right)^{1/2}} \frac{\partial \bar{u}}{\partial y}, \tag{1}$$

where m_1 and m_2 are material constants of Prandtl fluid model. As m_2 is nonzero due to fraction however m_1 can be any constant and for Newtonian fluid it can be zero. In the present model we incorporate the model of homogenous-heterogeneous reactions:

$$\left.\begin{array}{ll} A + 2B \rightarrow 3B, & \text{rate}=k_1 C_a C_b^2, \\ A \rightarrow B, & \text{rate}=k_2 C_a, \end{array}\right\} \tag{2}$$

where C_a and C_b denotes the concentration of the chemical species A and B, whereas k_1 and k_2 are the rate constants, respectively. After necessary boundary layer approximation the governing equations of our model may be written as follows:

$$\frac{\partial u}{\partial x} + \frac{\partial u}{\partial y} = 0, \tag{3}$$

$$u\frac{\partial u}{\partial x} + v\frac{\partial u}{\partial y} = u_\infty \frac{\partial u_\infty}{\partial x} + \frac{\vartheta m_1}{m_2}\frac{\partial^2 u}{\partial y^2} + \frac{\vartheta m_1}{2m_2^3}\left(\frac{\partial u}{\partial y}\right)^2 \frac{\partial^2 u}{\partial y^2} - \frac{\sigma B_0^2}{\rho}(u - u_\infty), \tag{4}$$

$$u\frac{\partial T}{\partial x} + v\frac{\partial T}{\partial y} = \alpha^*\left(\frac{\partial^2 T}{\partial y^2}\right) + \left(\frac{-\Delta H_h}{\delta_A}\right)\left(\frac{k_1 C_a C_b^2}{\rho C_p}\right), \tag{5}$$

$$u\frac{\partial C_a}{\partial x} + v\frac{\partial C_a}{\partial y} = D_A\frac{\partial^2 C_a}{\partial y^2} - k_1 C_a C_b^2, \tag{6}$$

$$u\frac{\partial C_b}{\partial x} + v\frac{\partial C_b}{\partial y} = D_B\frac{\partial^2 C_b}{\partial y^2} + k_1 C_a C_b^2, \tag{7}$$

with associated boundary conditions:

$$\left.\begin{array}{l} u = u_w(x) = cx, \quad v = 0, \quad -k_T\frac{\partial T}{\partial y} = k_2 C_a\left(\frac{-\Delta H_h}{\delta_A}\right), \\ D_A\frac{\partial C_a}{\partial y} = k_2 C_a, \quad D_B\frac{\partial C_b}{\partial y} = -k_2 C_a \end{array}\right\} \text{ at } y = 0$$
$$u \rightarrow u_\infty(x) = bx, \quad T \rightarrow T_\infty, \quad C_a \rightarrow C_\infty, \quad C_b \rightarrow 0 \quad \text{as } y \rightarrow \infty \tag{8}$$

where (u, v) is the usual notation for the cartesian coordinates velocity components, u_w is the velocity of stretching sheet, u_∞ is the ambient fluid velocity, T is the temperature of the fluid, T_w is the stretching sheet temperature, T_∞ is the ambient fluid temperature, density ρ of fluid, kinematic viscosity ϑ of the fluid, electrical conductivity σ of the fluid, thermal diffusivity α^* of the fluid, homogeneous heat reaction ΔH, Stoichiometric coefficient for heterogeneous reaction A of species, Diffusion coefficients of two species D_A and D_B, thermal conductivity k_T of the fluid, and a and b are dimensional constants. Introducing the following similarity transformations [14]:

$$f(\eta) = \frac{\psi}{x\sqrt{a\vartheta}}, \quad \theta(\eta) = \frac{T - T_\infty}{T_w - T_\infty}, \quad g(\eta) = \frac{C_a}{C_\infty}, \quad h(\eta) = \frac{C_b}{C_\infty}, \quad \eta = y\sqrt{\frac{a}{\vartheta}}. \tag{9}$$

where, stream function ψ is define in the form of $u = \partial\psi/\partial y$ and

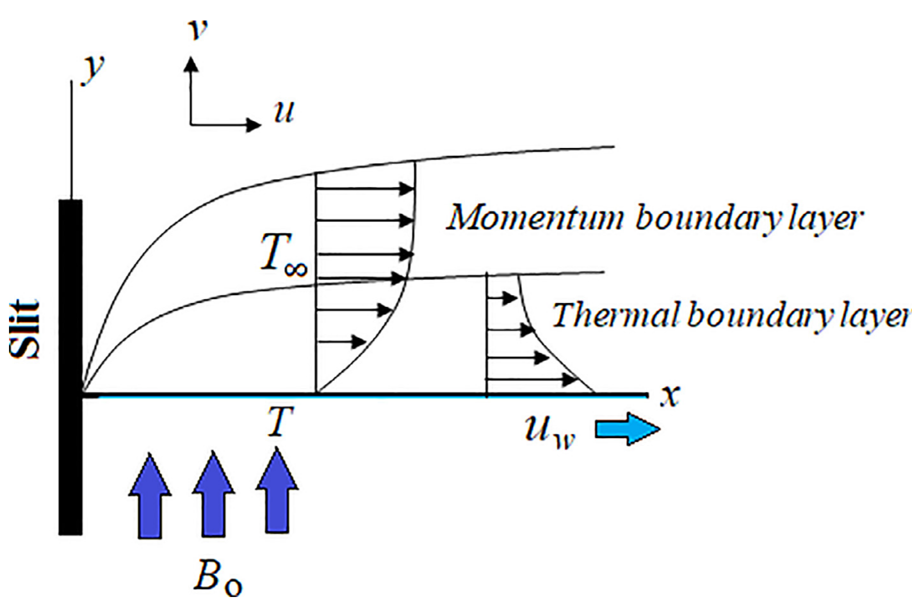

Fig. 1. Geometry of the model.

Table 1
Comparison of skin friction coefficient for stretching case (λ).

$\lambda\downarrow$	$M=0,\alpha=1,\beta=0$			
	Present results	Mahapatra and Nandy [23]	Wang [24]	Lok et al. [25]
0.0	1.2326	1.2326	1.2326	–
0.1	1.1466	1.1466	1.1466	
0.2	1.0511	1.0511	1.0511	
0.5	0.7133	0.7133	0.7133	0.7133
1.0	0	0	0	–
2.0	−1.8873	−1.8873	−1.8873	−1.8873
5.0	−10.2648	−10.2648	−10.2648	−10.2648

$v=-\partial\psi/\partial x$. It can be verified easily that equation of continuity (2) is identically satisfied and Eqs. (3) to (5) along with (6) take the following form:

$$\alpha f'''(\eta)+f(\eta)f''(\eta)-(f'(\eta))^2+\beta f'''(\eta)(f''(\eta))^2+M(r-f'(\eta))+r^2=0, \tag{10}$$

$$\frac{1}{\Pr}\theta''(\eta)+f(\eta)\theta'(\eta)+\gamma g(\eta)(h(\eta))^2=0, \tag{11}$$

$$\frac{1}{Sc}g''(\eta)+f(\eta)g'(\eta)-Kg(\eta)(h(\eta))^2=0, \tag{12}$$

$$\frac{\zeta}{Sc}h''(\eta)+f(\eta)h'(\eta)+Kg(\eta)(h(\eta))^2=0, \tag{13}$$

The dimensionless form of boundary conditions relative to the defined model is,

$$\left.\begin{array}{l} f(\eta=0)=0,\quad f'(\eta=0)=\lambda,\quad f'(\eta\to\infty)=r,\\ \theta'(\eta=0)=-K_T g(\eta=0),\quad \theta(\eta\to\infty)=0,\\ g'(\eta=0)=K_s g(\eta=0),\quad g(\eta\to\infty)=1,\\ \zeta h'(\eta=0)=-K_s g(\eta=0),\quad h(\eta\to\infty)=0, \end{array}\right\} \tag{14}$$

where, prime indicates the differentiation with respect to η, $\alpha=m_1/m_2$ is Prandtl fluid parameter, $\beta=a^3x^2m_1/2m_2^3\vartheta$ is elastic parameter, $M=\sigma B_0^2/\rho a$ is magnetic parameter, $r=b/a$ is the stagnation parameter, $\Pr=\vartheta/a$ is the Prandtl number, $\gamma=k_1(\Delta H_h/\delta_A)(1/\rho C_p)(C_\infty^3/a\Delta T)$ is the homogeneous reaction heat parameter, $Sc=\vartheta/D_A$ is the Schmidt number, $K=k_1C_\infty^2/a$ is the homogeneous reaction strength parameter, $\zeta=D_B/D_A$ is the ratio of diffusion coefficients, $\lambda=c/a$ is the stretching ($\lambda>0$) or shrinking ($\lambda<0$) parameter, $K_T=(k_2C_\infty/k_T\Delta T)(\Delta H_h/\delta_A)(a/\vartheta)^{1/2}$ is the thermal conductivity with respect to homogenous reaction and $K_S=k_2/D_A(a/\vartheta)^{1/2}$ is the heterogeneous reaction strength parameter.

We further consider the special case where diffusion coefficients of chemical species A and B are comparable. We assumed that diffusion coefficient D_A and D_B are equal, that is, $\zeta=1$. Hence we deduce the following identity.

$$g(\eta)+h(\eta)=1 \tag{15}$$

Using Eq. (15) in Eqs. (12)–(14) we get

$$\frac{1}{Sc}g''(\eta)+f(\eta)g'(\eta)-Kg(\eta)(1-g(\eta))^2=0, \tag{16}$$

Subject to the boundary conditions

$$g'(\eta=0)=K_S g(\eta=0),\quad g(\eta\to\infty)=1, \tag{17}$$

Expressions for skin friction coefficient C_f and local Nusselt number Nu are:

$$c_f=\frac{\tau_w}{\rho u_w^2},\quad Nu=\frac{xq_w}{k_T(T_w-T_\infty)}, \tag{18}$$

where, τ_w and q_w are the stress tensors and heat flux, respectively:

$$\tau=\frac{m_1}{m_2}\frac{\partial u}{\partial y}+\frac{m_1}{6m_2^3}\left(\frac{\partial u}{\partial y}\right)^3,\quad q_w=-k_T\left(\frac{\partial T}{\partial y}\right)_{y=0}, \tag{19}$$

Dimensionless form of Eq. (13) take the form:

$$\mathrm{Re}_x^{1/2}C_f=[\alpha f''(\eta)+\beta(f''(\eta))^3]_{\eta=0},\quad \mathrm{Re}_x^{-1/2}Nu=-\theta'(0). \tag{20}$$

where, $\mathrm{Re}_x=\frac{u_w x}{\vartheta}$ is local Reynolds number based on the stretching velocity $u_w(x)$.

Numerical procedure

Numerical experiment is performed over non-linear coupled ordinary differential Eqs. (10)–(13) along with boundary conditions (14) using Finite Difference Scheme called Keller Box Method [21]. The method is second-order accurate and discretizes the given non-linear ordinary differential equation into the system of first-order differential equations. Newton's iteration method is used to counter the non-linearity of the equation. The resulting linear system is solved using any block-tridiagonal procedure. The method has been applied successfully to solve the non-linear coupled differential equations by Soomro et al. [22]. In present simulation the uniform step size of 10^{-4} and truncation error tolerance of 10^{-8} was used. After initial experimental analysis it was concluded to restrict the infinite domain to $\eta=[0, 8]$ to show the convergence of the solution profiles. Results are validated through numerical values of skin friction coefficient with previous published work mentioned in Table 1.

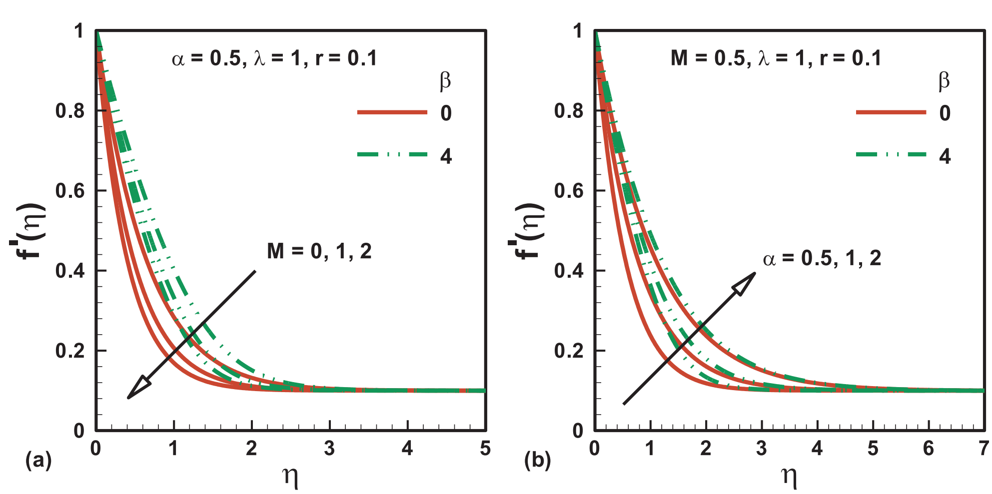

Fig. 2. Effects of physical parameters (a) M and (b) α on velocity when $\beta=0$ and $\beta=4$.

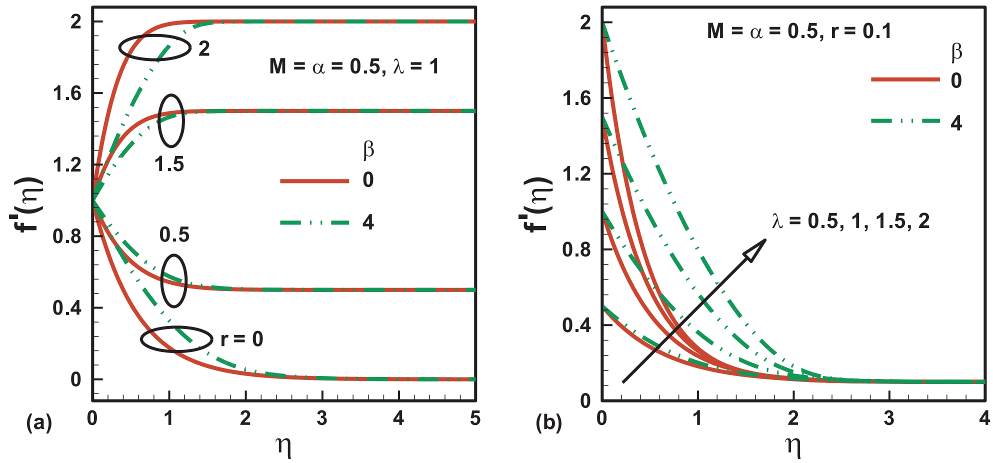

Fig. 3. Effects of physical parameters (a) r and (b) λ on velocity when $\beta = 0$ and $\beta = 4$.

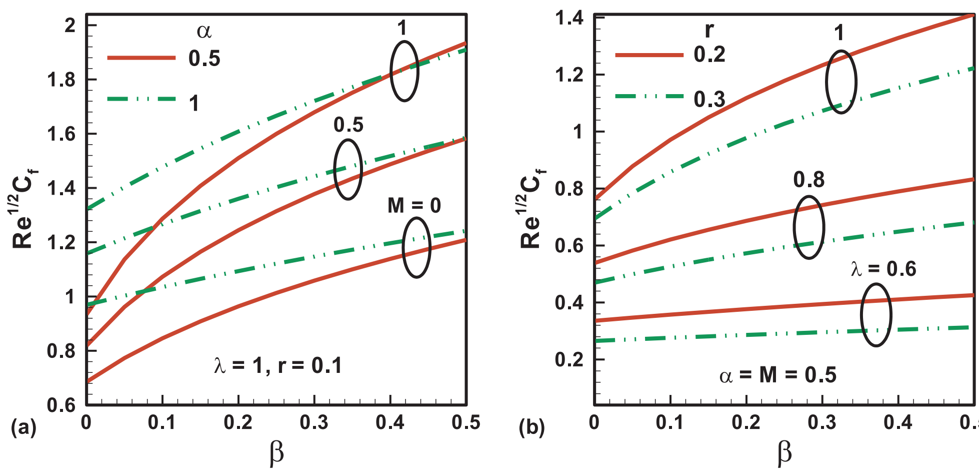

Fig. 4. Effects of physical parameters on coefficient of skin friction.

Results and discussion

Effects on velocity profiles

Figs. 2 and 3 describe the nanofluid velocity change due to variation in pertinent physical parameters. It can be seen from profiles trend that increase in Prandtl fluid parameter, stagnation parameter and stretching parameter enhances the nanofluid velocity. It should be noted that increase in elastic parameter also enhances nanofluid velocity when $r = 1$. Moreover, Fig. 3(a) shows that, there is different effect on the nanofluid velocity for different range of stagnation parameter. It is observed that, due to increase in elastic parameter, nanofluid velocity decreases when $r > 1$ whereas it enhances when $r < 1$. Increase in magnetic parameter has decreasing effect on the nanofluid velocity (Fig. 2(a)). Thermal boundary layer thickness of nanofluid decrease due to increase in magnetic parameter, elastic parameter and stretching parameter. On the other hand, no significant effect on the velocity boundary layer thickness is seen due to variation in stagnation parameter.

Effects on coefficient of skin friction

Impact of emerging physical parameters on the coefficient of skin friction can be seen from the Fig. 4. Skin friction increases due to increase in Prandtl fluid parameter, elastic parameter, stretching parameter and magnetic parameter. On the other hand it tends to decrease due to increase in stagnation parameter. Furthermore, it is observed from Fig. 4(b) that at comparatively high stagnation parameter value the skin friction value tends to increase at higher rate due to increase in elastic parameter. The behavior is vice versa for comparatively low value of stagnation parameter.

Effects on temperature

Fluid temperature distribution due to variation in contained physical parameters is depicted through Fig. 5. Temperature of fluid tends to enhance due to increase in the value of magnetic parameter, thermal conductivity parameter and homogeneous reaction parameter. On the other hand, decreasing effect is observed on the fluid temperature due to increase in Prandtl number, Prandtl fluid parameter and elastic parameter. Moreover, thermal boundary layer thickness tends to decrease due to increase in magnetic parameter, elastic parameter, Prandtl number and Prandtl fluid parameter. On the other hand, thermal boundary layer thickness increases due to increase in homogeneous reaction parameter and thermal conductivity parameter.

Effects on Nusselt number

Due to increment in various physical parameters the effects on the Nusselt number can be seen from Fig. 6. Heat transfer rate tends to decrease due to increase in magnetic parameter, homogeneous reaction stretching parameter and heterogeneous reaction strength parameter.

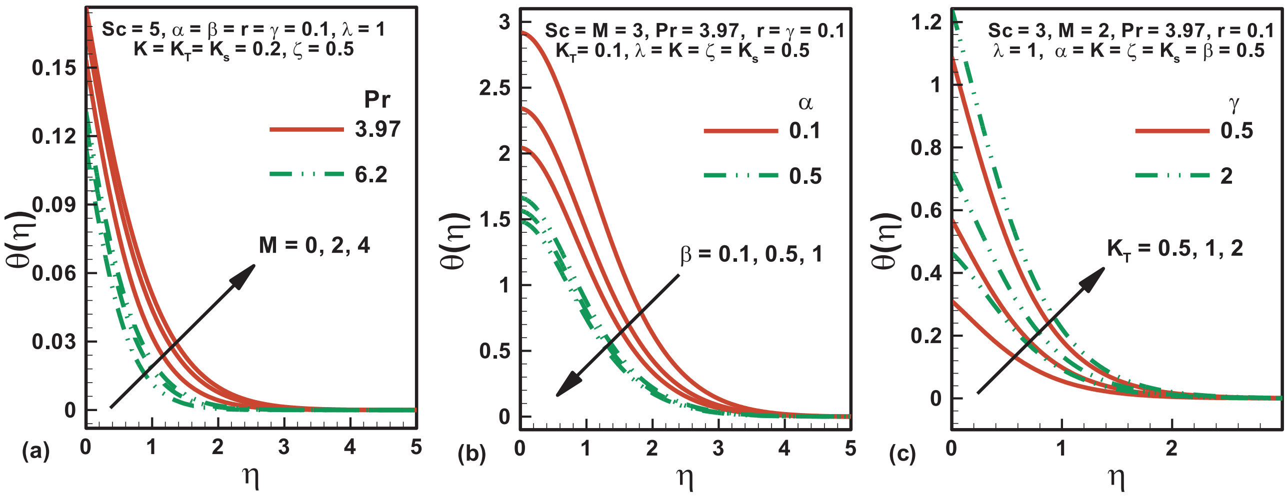

Fig. 5. Effects of physical parameters (a) Hartmann number, (b) elastic parameter and (c) conductivity with respect to homogenous reaction on temperature profile.

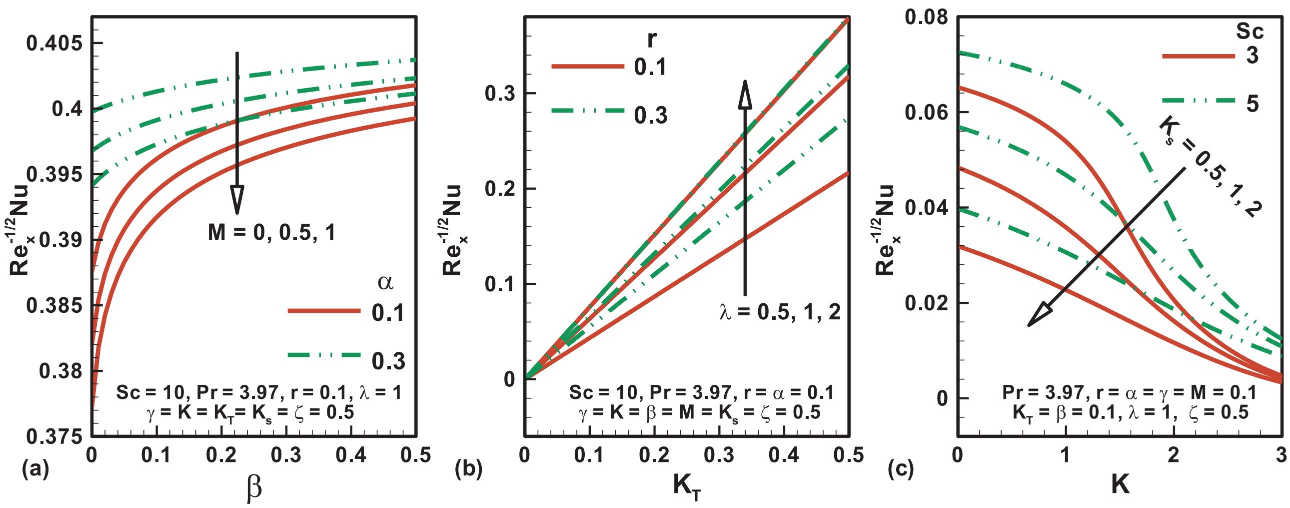

Fig. 6. Effects of physical parameters on Nusselt number.

On the other hand, due to increment in Prandtl fluid parameter, elastic parameter, stagnation parameter, thermal conductivity parameter and Schmidt number the Nusselt number tends to increase.

Conclusion

Non-Newtonian Prandtl fluid stagnation-point nanofluid fluid flow under the homogeneous-heterogeneous reactions was analyzed in present research work. The physical problem was modeled into the mathematical form in terms of partial differential equations which were transformed into the set of nonlinear ordinary differential equations using similarity transformations. Finite Difference Method was utilized to seek the numerical solution of such set of equations. Nanofluid velocity, skin friction, temperature distribution and heat transfer rate was analyzed against the varying value so the emerging physical parameters. It was observed that increase in homogeneous and heterogeneous reaction strength decreases the heat transfer rate. Increase in thermal conductivity due to homogeneous reactions enhances the heat transfer rate. As a result more temperature is transferred to the surrounding fluid which enhances its temperature.

Acknowledgements

The first author is thankful to the National Science Foundation of China for research support having grant number 11271187.

References

[1] Irgens F. Rheology and non-Newtonian fluids. Springer; 2014.
[2] Khan M, Ahmad L, Khan WA, Alshomrani AS, ALzahrani AK, Alghamdi MS. A 3D Sisko fluid flow with Cattaneo-Christov heat flux model and heterogeneous-homogeneous reactions: a numerical study. J Mol Liq 2017;238:19–26.
[3] Besthapu P, Haq RU, Bandari S, Al-Mdallal QM. Thermal radiation and slip effects on MHD stagnation point flow of non-Newtonian nanofluid over a convective stretching surface. Neural Comput Appl 2017. http://dx.doi.org/10.1007/s00521-017-2992-x.
[4] Usman M, Soomro FA, Haq RU, Wang W, Defterli O. Thermal and velocity slip effects on Casson nanofluid flow over an inclined permeable stretching cylinder via collocation method. Int J Heat Mass Transf 2018;122:1255–63.
[5] Akbar NS, Nadeem S, Haq RU, Ye SW. MHD stagnation point flow of Carreau fluid towards a permeable shrinking sheet: dual solutions. Ain Shams Eng J 2014;5:1233–9.
[6] Nadeem S, Haq RU, Khan ZH. Numerical study of MHD boundary layer flow of a Maxwell fluid past a stretching sheet in the presence of nanoparticles. J Taiwan Inst Chem Eng 2014;45:121–6.
[7] Akbar NS, Nadeem S, Lee CH, Khan ZH, Haq RU. Numerical study of Williamson nano fluid flow in a asymmetric channel. Results Phys 2013;3:161–6.
[8] Zhang Y, Zhang M, Bai Y. Flow and heat transfer of an Oldroyd-B nanofluid thin film over an unsteady stretching sheet. J Mol Liq 2016;220:665–70.
[9] Rehman SU, Haq RU, Khan ZH, Lee CH. Entropy generation analysis for non-Newtonian nanofluid with zero normal flux of nanoparticles at the stretching surface. J Taiwan Inst Chem Eng 2016;63:226–35.
[10] Sajid M, Ahmad I, Hayat T, Ayub M. Unsteady flow and heat transfer of a second grade fluid over a stretching sheet. Commun Nonlinear Sci Numer Simul 2009;14:96–108.
[11] Akbar NS, Khan ZH, Haq RU, Nadeem S. Dual solutins in MHD stagnation-point flow of Prandtl fluid impinging on shrinking sheet. Appl Math Mech

2014;35:813–20.
[12] Soomro FA, Haq RU, Khan ZH, Zhang Q. Passive control of nanoparticles due to convective heat transfer of Prandtl fluid model at the stretching surface. Chin J Phys 2017;55:1561–8.
[13] Ganesh K, Haq RU, Rudraswamy NG, Gireesha BJ. Effects of mass transfer on MHD three dimensional flow of a Prandtl liquid over a flat plate in the presense of chemical reaction. Results Phys 2017;7:3465–71.
[14] Chaudhary MA, Merkin JH. A simple isothermal model for homogeneous-heterogeneous reactions in boundary-layer flow. I Equal diffusivities. Fluid Dyn 1995;16:311–33.
[15] Khan MI, Waqas M, Hayat T, Alsaedi A. A comparative study of Casson fluid with homogeneous-heterogeneous reactions. J Colloid Interface Sci 2017;498:85–90.
[16] Ramzan M, Bilal M, Chung JD. MHD stagnation point Cattaneo-Christov heat flux in Williamson fluid flow with homogenous-heterogeneous reactions and convective boundary condition – a numerical approach. J Mol Liq 2017;225:856–62.
[17] Hayat T, Hussain Z, Alsaedi A, Mustafa M. Nanofluid flow through a porous space with convective conditions and heterogeneous-homogeneous reactions. J Taiwan Inst Chem Eng 2017;70:119–26.
[18] Khan I, Malik MY, Hussain A, Salahuddin T. Effect of homogenous-heterogeneous reactions on MHD Prandtl fluid flow over a stretching sheet. Results Phys 2017;7:4226–31.
[19] Abbas Z, Sheikh M. Numerical study of homogeneous-heterogeneous reactions on stagnation point flow of ferrofluid with non-linear slip condition. Chin J Chem Eng 2017;25:11–7.
[20] Hayat T, Khan MI, Alsaedi A, Khan MI. Homogeneous-heterogeneous reactions and melting heat transfer effects in the MHD flow by a stretching surface with variable thickness. J Mol Liq 2016;223:960–8.
[21] Keller HB. A new difference scheme for parabolic problems in “Numerical solution of partial differential equations.” J. Bramble Edition, Volume II. New York: Academic Press; 1970.
[22] Soomro FA, Haq RU, Khan ZH, Zhang Q. Numerical study of entropy generation in MHD water-based carbon nanotubes along an inclined permeable surface. Eur Phys J Plus 2017;132:412.
[23] Mahapatra TR, Nandy SK. Stability of dual solutions in stagnation-point flow and heat transfer over a porous shrinking sheet with thermal radiation. Meccanica 2013;48:23–32.
[24] Wang CY. Stagnation flow towards a shrinking sheet. Int J Non Linear Mech 2008;43:377–82.
[25] Lok YY, Amin N, Pop I. Non-orthogonal stagnation point towards a stretching sheet. Int J Non Linear Mech 2006;41:622–7.